Supplementary information

Unusual Slow Magnetic Relaxation in a Mononuclear Copper(II) Complex

Dušan Valigura, Cyril Rajnák,* Ján Titiš, Ján Moncoľ, Alina Bieńko, Roman Boča

Preparation of complex [CuLL'$_2$(H_2O)], **1**, where L = 2,6-dimethanolpyridine, L' = 3,5-dinitrocarboxylate(1-), is based upon following recipe. A solution of copper(II) acetate dissolved in 20 ml of water and poured to 20 ml of aqueous solution of 2,6-pyridinedimethanol (1 mmol) and 2 mmol of 3,5-dinitrobenzoic acid was added to the reaction mixture under stirring at laboratory temperature until color stabilization and left to crystallize. The green crystals, formed within 4 weeks, were filtered, washed with small amount of water and dried in air at ambient temperature. Anal Calc for**1**: N, 10.89; C, 39.23; H, 2.66. Found: N, 10.60; C, 40.67; H, 2.92 %.

CHNS analyzer (Thermo Scientific, Flash 2000) was used for elemental analysis (EA). For FT-IR (ATR) spectra freshly grown crystals were used. The UV/Vis absorption spectra in the range 190 – 1100 nm were measured at room temperature in the Nujol suspension (Analytical Jena, Specord 250 Plus). Commercial desktop EPR spectrometer was used (ESR-5000, Margitech/Bruker) in taking the X-band powder EPR spectra at the room temperature.

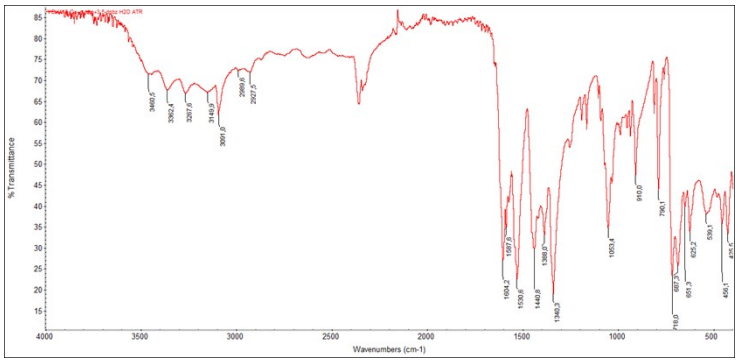

Figure S1. FT-IR spectrum of **1**.

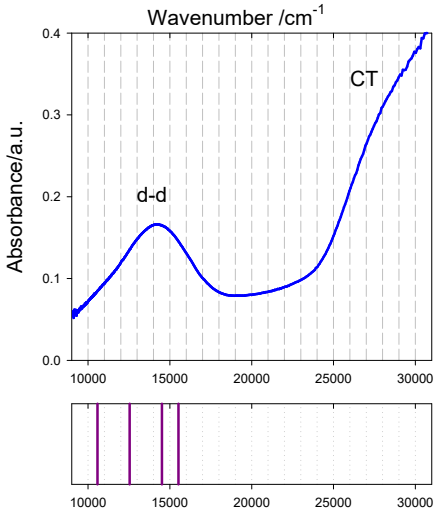

Figure S2. UV/Vis spectrum of **1**, band maximum at 14276 cm^{-1}. Calculated d-d transitions – bars.

In octahedral Cu(II) complexes the ground electronic term is ^2E_g, which is, however, a hypothetical case, since Jahn-Teller (JT) effect applies causing tetragonal and/or rhombic distortions. In the studied Cu(II) complex, SA-CAS[9,5]/NEVPT2 calculated first excited term lies at ~10 508 cm^{-1} ($^2B_{1g} \rightarrow {}^2A_{1g}$ in D_{4h}) as a consequence of the strong JT splitting. The remaining transitions are predicted at 12544, 14517, and 15524 cm^{-1}.

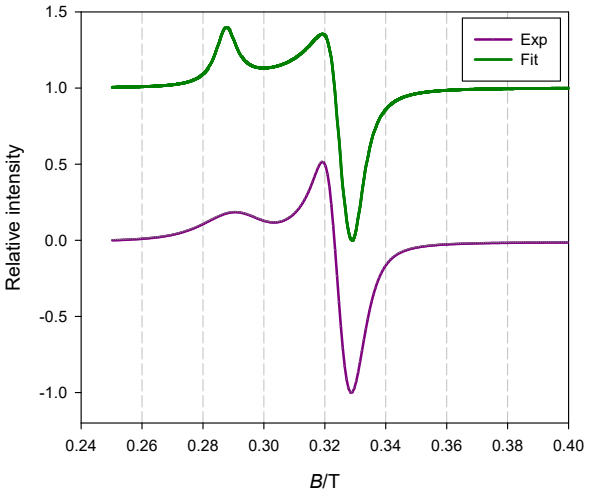

Figure S3. X-band (9.4457 GHz) EPR spectrum of **1** at room temperature. Simulation for a mononuclear species with $S = 1/2$: $\boldsymbol{g}\{2.050(1), 2.083(1), 2.347(3)\}$.

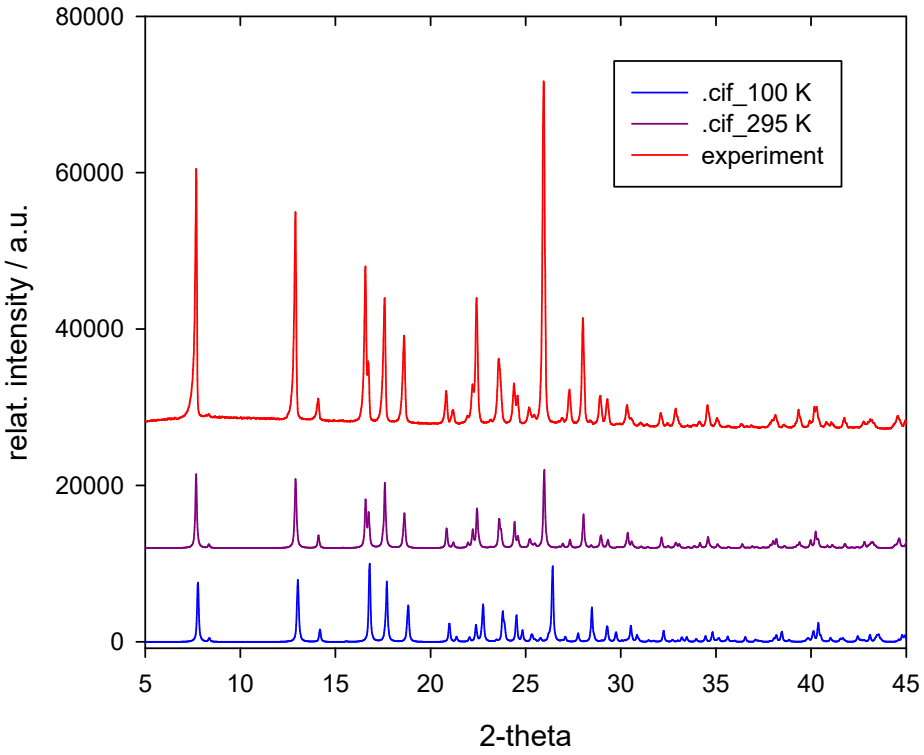

Figure S4. Powder diffraction patterns for **1**.

Table S1. Crystal data and structure refinement for **1**.

	1	**1'**
Empirical formula	$C_{21}H_{17}CuN_5O_{15}$	$C_{21}H_{17}CuN_5O_{15}$
Formula weight /g mol^{-1}	642.93	642.93
Crystal system	monoclinic	monoclinic
Space group	*C*2/c	*C*2/c
Temperature /K	100	295
Crystal size /mm	0.26 × 0.03 × 0.02	0.56 × 0.37 × 0.18
Z	4	4
a / Å	21.1052(11)	21.1547(4)
b / Å	13.4854(4)	13.7108(3)
c / Å	8.4582(4)	8.5157(1)
α /°	90	90
β /°	90.366(4)	90.397(1)
γ /°	90	90
V /Å^3	2407.26(18)	2469.90(8)
ρ_{calc} /g cm^{-3}	1.774	1.729
μ /mm^{-1}	2.126	0.970
F(000)	1208.0	1308.0
Radiation	CuKα (λ = 1.54186)	MoKα (λ = 0.71069)
2Θ range for data collection/°	7.78 to 143.594	6.498 to 59.184
Index ranges	-18 ≤ h ≤ 25, -16 ≤ k ≤ 13, -7 ≤ l ≤ 10	-29 ≤ h ≤ 29, -18 ≤ k ≤ 18, -11 ≤ l ≤ 11
Data/restraints/parameters	2319/6/196	3303/6/197
Goodness-of-fit on F^2	1.057	1.073
Final R indexes [I >= 2σ (I)]	R_1 = 0.0292, wR_2 = 0.0795	R_1 = 0.0324, wR_2 = 0.0857
R indices (all data)	R_1 = 0.0360, wR_2 = 0.0818	R_1 = 0.0523, wR_2 = 0.0945
color	blue	blue
CCDC No.	2065544	2065545

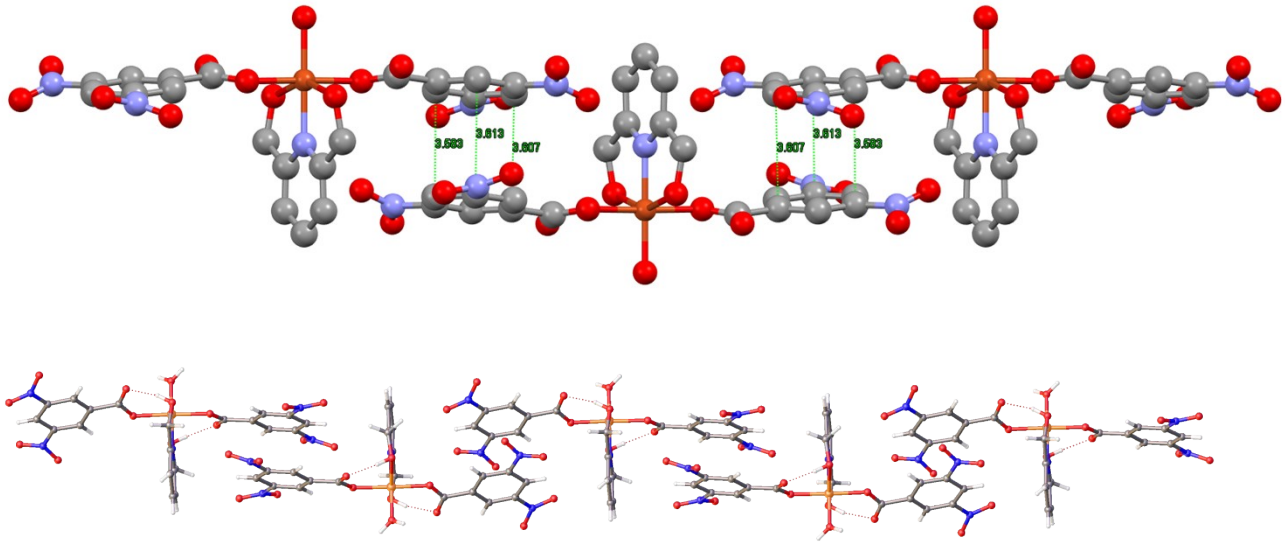

Figure S5. A more detailed view to the intermolecular π–π stacking in **1** (top) and view of the supramolecular chain formed through π–π stacking interactions [centroid-centroid distance: 3.601 Å, shift distance: 1.144 Å] (bottom).

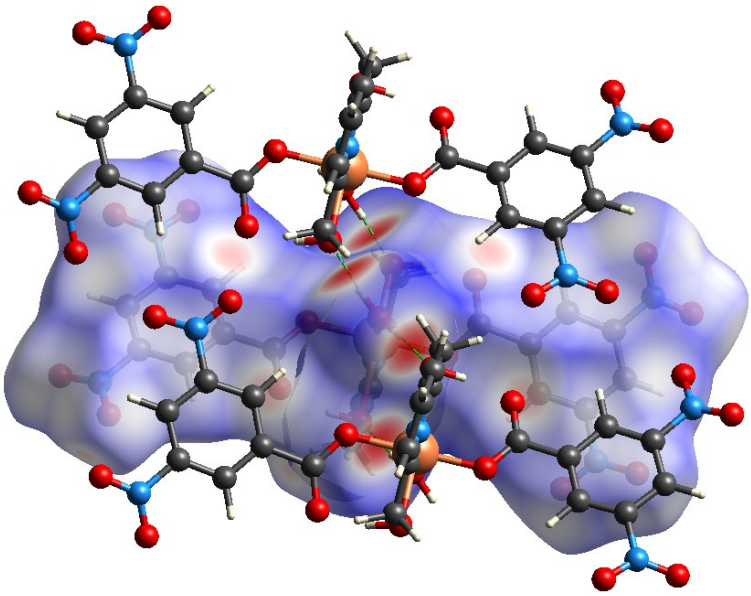

Figure S6. View of the three-dimensional Hirshfeld surface of **1** plotted over d_{norm} in the range -0.7248 to 1.3175 a.u. Red spots show close contacts.

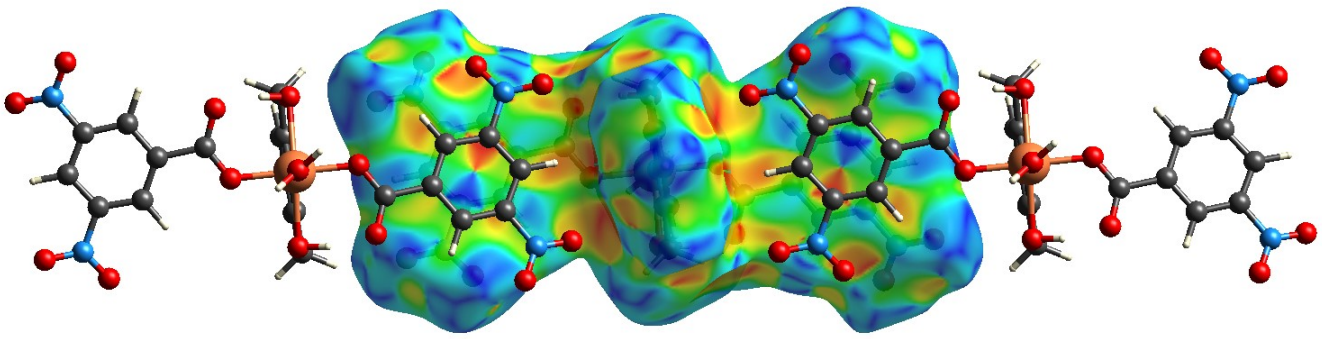

Figure S7. View of the three-dimensional Hirshfeld surface of **1** plotted over shape index showing π-π stacking interactions.

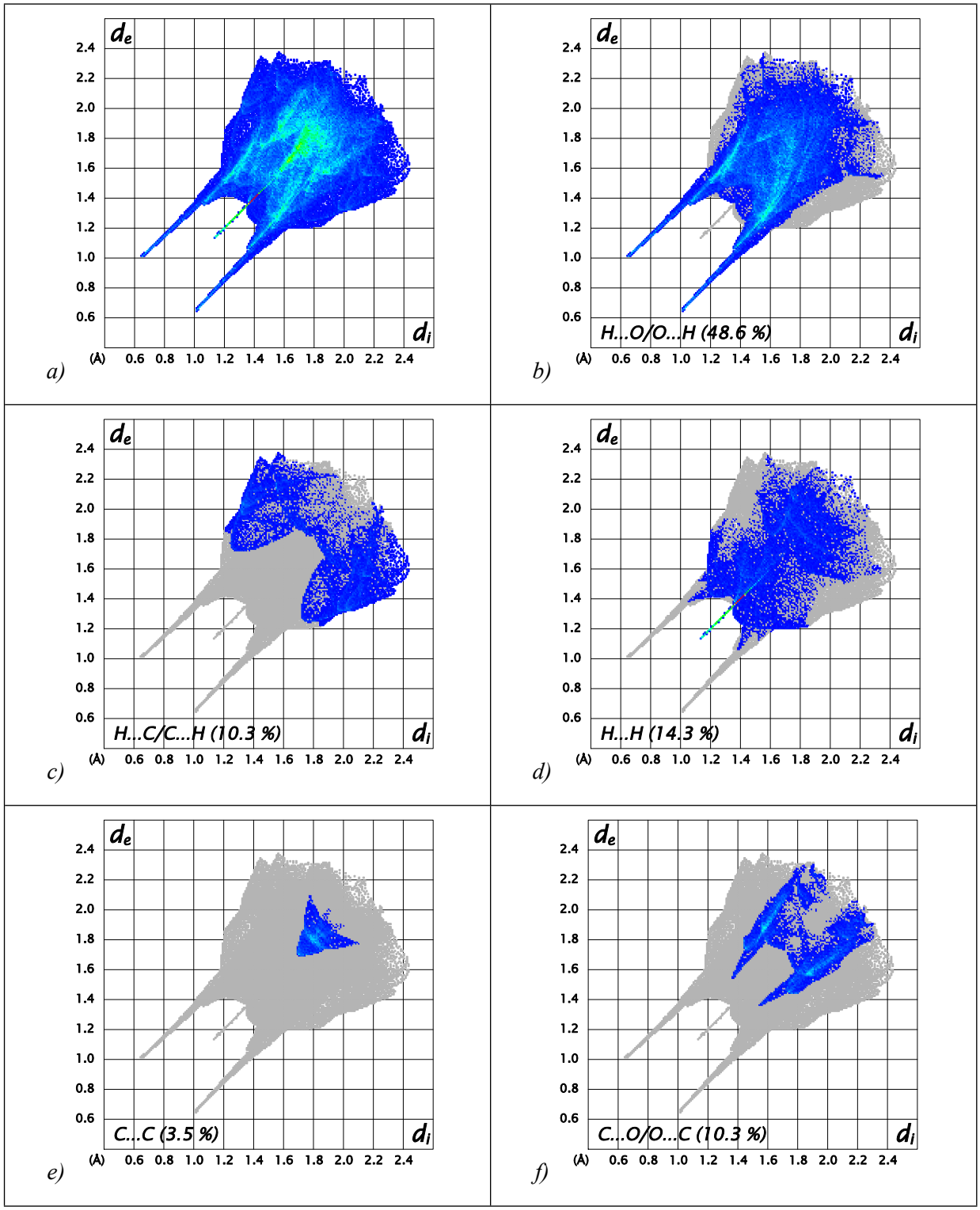

Figure S8. The full two-dimensional fingerprint plots of **1** (at 100K), showing (*a*) all interactions, and delineated into (*b*) H···O/O···H, (*c*) H···C/C···H, (*d*) H···H, (*e*) C···C, and (*f*) C···O/O···C interactions. The d_i and d_e values are the closest internal and external distances from given on the Hirshfeld surface contacts.

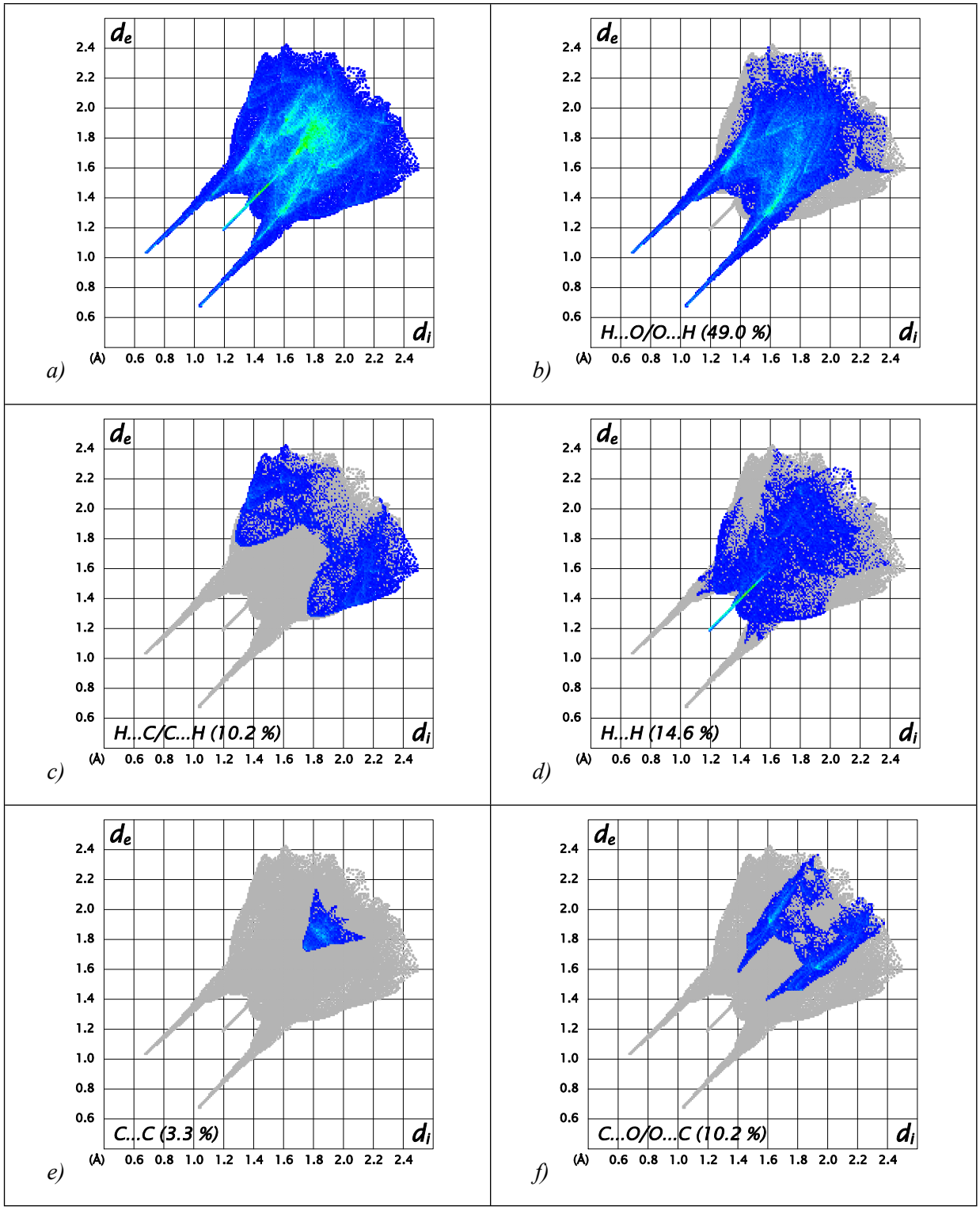

Figure S9. The full two-dimensional fingerprint plots of **1** (at 295K), showing (*a*) all interactions, and delineated into (*b*) H···O/O···H, (*c*) H···C/C···H, (*d*) H···H, (*e*) C···C, and (*f*) C···O/O···C interactions. The d_i and d_e values are the closest internal and external distances from given on the Hirshfeld surface contacts.

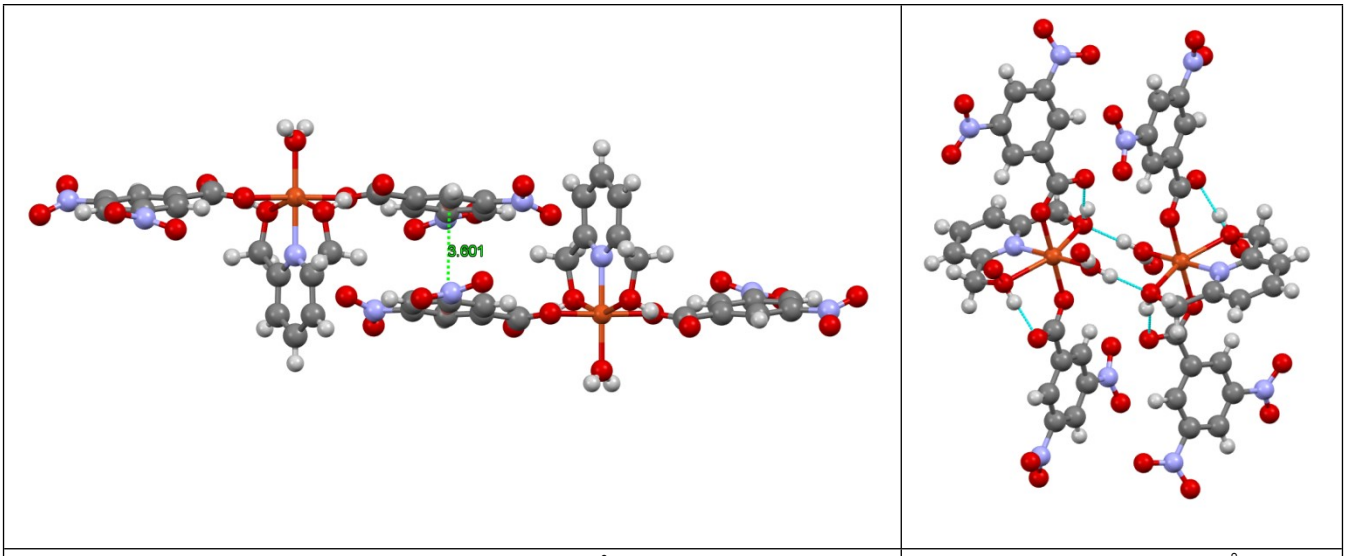

π–π stacking (Cu...Cu ~12 Å), $J_{\pi-\pi}$ = +1.14 cm^{-1}	H-bond (Cu...Cu ~5 Å), $J_{\text{H-bond}}$ = +0.68 cm^{-1}

Figure S10. Model dimers for DFT calculations.

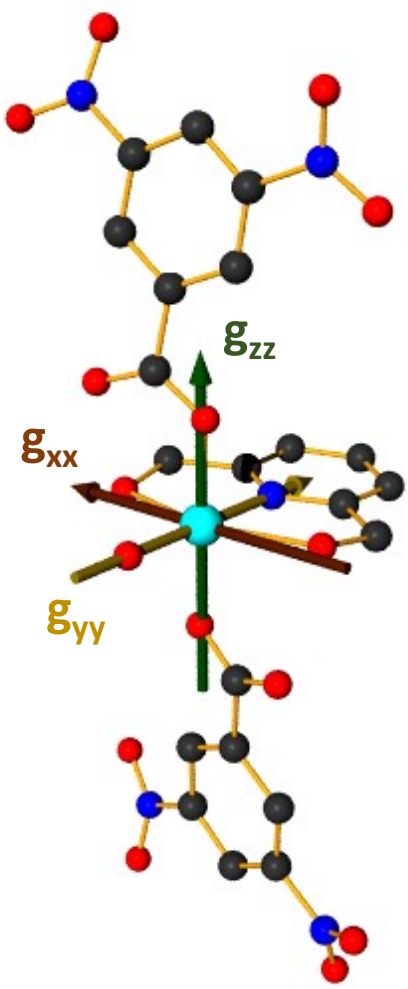

Fig. S11. Molecular structure of **1** along with the visualization of the calculated g-tensor componets in the crystallographic molecular frame.

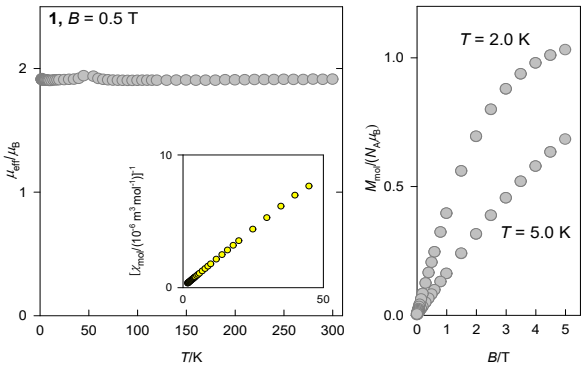

Figure S12. DC magnetic data.

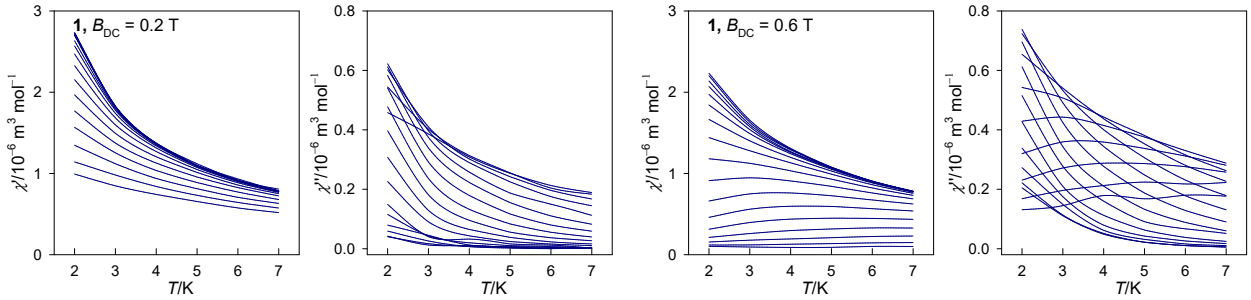

Figure S13. Temperature evolution of the AC susceptibility for **1**.

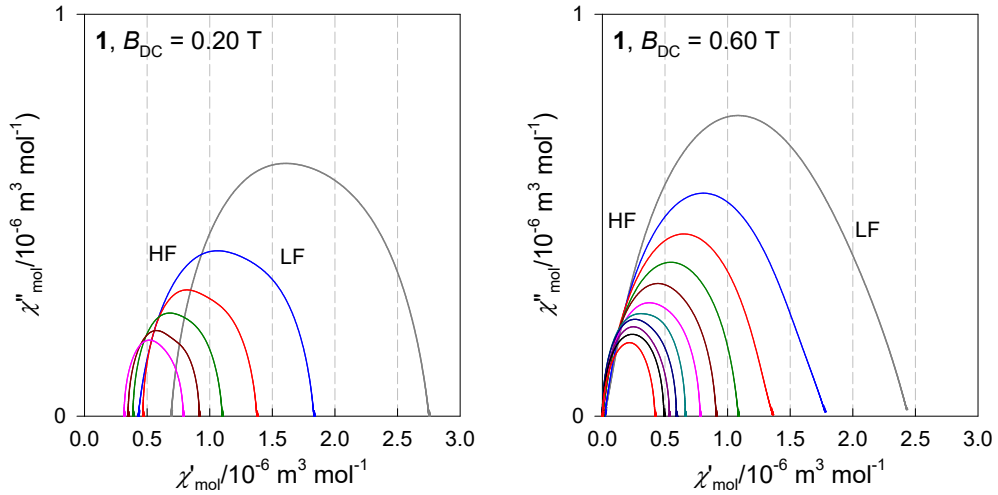

Figure S14. Cole-Cole plots for **1** showing an asymmetry due to merged two arcs.

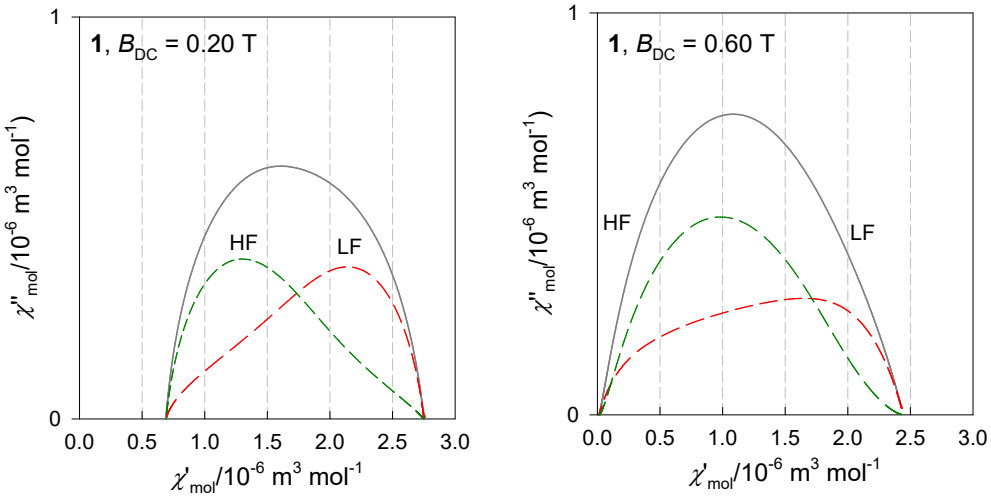

Figure S15. Decomposition of the Cole-Cole plots for **1** to two relaxation channels.